Flow control on a high thickness airfoil by a trapped vortex cavity.

Fabrizio De Gregorio[1] , Giuseppe Fraioli[2]

1: LMSA/IWTU laboratory, Centro Italiano Ricerche Aerospaziali (CIRA), Capua, Italy, f.degregorio@cira.it
2: Dept. Mechanics and Aeronautics, University of Rome "La Sapienza", Rome, Italy, giuseppe_fraioli@hotmail.it

Abstract This paper summarises the experimental campaign performed at CIRA CT-1 wind tunnel aimed to investigate the potential benefit obtainable using a trapping vortex cell system on a high thickness airfoil with and without steady suction and/or injection mass flow.
The behaviour of a 2D model, equipped with a span wise oriented circular cavity, has been investigated. Pressure distribution on the model surface and inside the cavity and the complete flow field around the model and inside the cavity have been measured.
An extensive test campaign has been carried out in the CT-1, an open circuit wind tunnel, with test section size of 305x305x600 mm^3 and maximum speed of 55 m/s. Due to the limited dimensions of the WT, the model has been mounted on the bottom wall of the wind tunnel in order to avoid blockage problems. The model represents a two dimensional high thickness airfoil with a chord length of 350mm. The model angle of attack ranges between 5.66° to 12.66° with a step of 1°.
The installation of the model on the wind tunnel bottom wall presented heavy flow instability under the front part of the model. The flow instability has been solved applying a flow suction in front the model trough a porous wall installed on the bottom WT wall. The cavity has been realized with transparent material in order to allow optical access and consequently PIV measurements. The model has been designed in order to permit flow suction and/or blowing inside the cavity.
The influence of different parameters has been investigated. Tests have been performed varying the wind tunnel speed (form 15 m/s, to 30 m/s), varying the suction mass flow (from 0 m^3/h to 25 m^3/h) varying the blowing mass flow (from 0 m^3/h to 50 m^3/h) applying suction and blowing at the same time, and varying the model angle of attack (AoA).
In the paper the performed test campaign, the adopted experimental set-up, the data post-processing and the results' description are reported.

1. Introduction

To ensure an high lift-to-drag ratio, wing of modern airplanes are thin and streamlined. However the tendency to design commercial aircraft of ever-larger dimensions, or innovative configuration as Blended-Wing-Body airplanes requests innovative solution in the field of wing structures. In order to carry a larger load having thick wing would be beneficial. The drawback of this type of airfoils is a low efficiency due to high value of the drag coefficient. These airfoils are affected by early flow separation phenomenon even for small incidence angle.

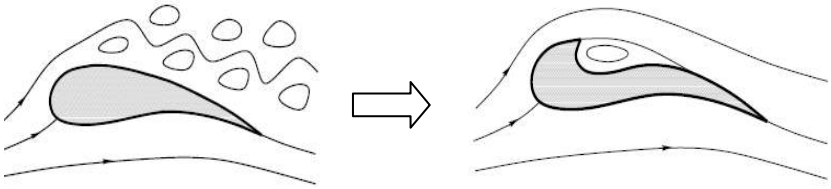

Figure 1: Trapped vortex concept

Nowadays many research activities are aimed to investigate system dedicated to flow control. As a scientific discipline and as a technological curiosity, flow control is perhaps more hotly pursued by scientists and engineers than any other area in fluid mechanics (see Gad-el Hak 1996).

Flow control involves passive or active devices to effect a beneficial change in wall bounded or free-shear flows.
The ability to manipulate a flow field to effect a desired change is of immense practical importance.
An external wall-bounded flow, such as that developing on the exterior surface of an aircraft or a submarine, can be manipulated to achieve transition delay, separation postponement, lift increase, skin-friction and pressure drag reduction, turbulence augmentation, heat transfer enhancement, or noise suppression. By preventing separation, lift is enhanced, stall is delayed, pressure recovery is improved and form drag is reduced. The challenge in choosing a flow control scheme is of course to achieve a beneficial goal at a minimum cost, without adversely affecting another goal. An ideal method of control that is simple, is inexpensive to build and to operate, and does not have any trade-off does not exist, and the skilled engineer has to make continuous compromises to achieve a particular design objective.
There are different classification schemes for flow control methods. One is to consider whether the technique is applied at the wall or away from it, we shall deal with the first one. Surface parameters that can influence the flow include roughness, shape, curvature, rigid-wall motion, temperature, and porosity. Heating and cooling of the surface can influence the flow via the resulting viscosity and density gradients. Mass transfer can take place through a porous wall or a wall with slots. Suction and injection of primary fluid can have significant effects on the flow field, influencing particularly the shape of the velocity profile near the wall and thus the boundary layer susceptibility to transition and separation. Momentum transfer by synthetic jet actuators or plasma actuators operates as well on the flow field energising the boundary layer.
A second scheme for classifying flow control methods considers energy expenditure and the control loop involved. A control device can be passive, requiring no auxiliary power, or active, requiring energy expenditure. Active control is further divided into predetermined or reactive. Predetermined control includes the application of steady or unsteady energy input without regard to the particular state of the flow. The control loop in this case is open, and no sensors are required. Reactive control is a special class of active control where the control input is continuously adjusted based on measurements of some kind. The control loop in this case can either be an open, feedforward one or a closed, feedback loop. Classical control theory deals, for the most part, with reactive control.
Future possibilities for aeronautical applications of flow separation control include providing structurally efficient alternatives to flaps or slats; cruise application on conventional takeoff and landing aircraft including boundary-layer control (BLC) on thick spanloader wings; as well as cruise application on high-speed civil transports for favorable interference wave-drag reduction, increased leadingedge thrust, and enhanced fuselage and upper surface lift. In fact, much of the remaining gains to be made in aerodynamics appear to involve various types of flow control, including separated flow control. Typical, in some cases serious, problems associated with flow separation control include parasitic device drag or energy consumption; system weight, volume, complexity, reliability or cost; performance sensitivity to body attitude or orientation.
At the end of 2005, VortexCell2050, an European research project, has been launched with the scope of investigate the possibility to control the flow separation using trapped vortex cavities and active control.
Basic concept of the trapped vortex cavities (TVC) is shown in figure 1. The flow otherwise separated is forced to remain attached by an intense vortex anchored in the cavity. One of the critical point is to maintain the vortex stable in the cavity, and with a sufficient strength to forcing the flow reattachment. The idea of trapping a vortex is old, and it is not easy to find out who first suggested it (Ringleb F.O. 1961). A trapped vortex could be just a steady separation eddy above an aerofoil at high angle of attack, but the use of a vortex cell helps. Practical implementation of the trapped-vortex idea is tricky, since the trapped vortex needs to be almost steady in the sense that it should remain in the close vicinity of the body. The first successful use of a trapped vortex in a flight experiment was claimed by W.A.Kasper in the seventies with is well know wing. Figure 2

shows the ideal concept of the Kaspar wing. Experimental tests aimed to verify the Kaspar wing behaviour (Kruppa in 1977) showed the presence of vortex shedding instead of steady vortex and any lift enouncement was observed. The same Kruppa reported in his paper some promising results obtained by researchers of Saab-Scania (1974) on a wing presenting a vortex cavity and blowing applying flow injection in the cavity (figure 3).

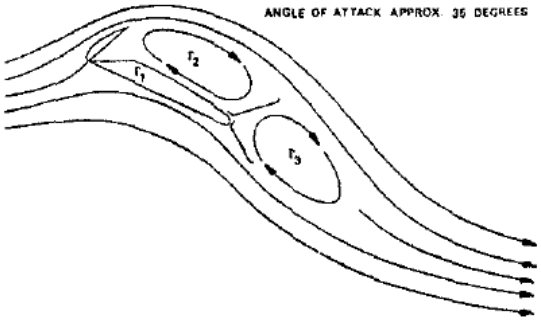

Figure 2: Kasper wing concept

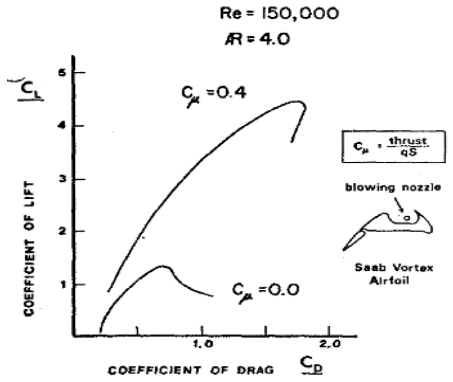

Figure 3: Saab vortex airfoil

The potential advantage to use TVC is that the presence of the cavity on the wing surface naturally induces the vortex formation inducing flow reattachment requiring no auxiliary power. But the analysis of the few available data shows that stable flows with trapped vortex are rare, for this reason an active flow control is necessary, but the energy expenditure should be limited.
For gaining a better understanding of the impact of TVC on an airfoil and overcome the lack of experimental data an extensive test campaign has been performed. In order to maintain low the cost of the basic investigations, the measurements have been performed in the small CT-1 wind tunnel (WT). Furthermore, the necessity to mount the trapped cavities and to simulate a Reynolds' number up to one million requested to built a model with a chord length of at least 350mm. For fulfil the above mentioned requeriments and install the model in the CT-1 avoiding blockage problems, the model has been mounted on the bottom wall of the wind tunnel. A first measurement campaign has been carried out for characterising the flow and pressure distribution behaviour of a clean high thick airfoil. The tests were mainly focused to characterise the flow separation behaviour for different test conditions (De Gregorio F. and others. 2007). Once the aerodynamic characteristics of the clean airfoil have been detected, the behaviour of the airfoil housing a trapped vortex cavity has been investigated. A second test campaign has been aimed to investigate the influence on the airfoil aerodynamic of passive/active TVC flow control, i.e. without/with steady suction and/or injection inside the cavity. The tests have foreseen pressure and flow field measurements on the model surface and inside the cavity. This second test activity is the object of this work. As future activity, the project foresees to test the TVC system on a two dimensional model in a large wind tunnel in order to evaluate the benefit in terms of efficiency.

2. Experimental apparatus

The experimental apparatus, including the test facility, test models and instrumentation are described in the following.

2.1 Test facility

The tests have been carried out in the CT-1 (fig.4), an open circuit wind tunnel, with test section size of 305x305x600 mm^3, maximum speed of 55 m/s, nozzle contraction rate of 16:1 and maximum value of turbulence level at 50 m/s flow speed of 0.1%.
The wind tunnel bottom has been modified in order to accommodate the model. Furthermore the

peculiar configuration showed intense flow instability due to the formation of a strong re-circulating zone located under the leading edge of the model. In order to reduce the flow unsteadiness, flow suction is applied in front the test article, in concomitance of the circulation region, in order to confine/eliminate the circulation zone and neglect vortex shedding along the model. Figure 5 provides a detailed view of test section with the model mounted on the bottom wall and the adopted reference system. Two porous plates, with a solidity ratio of 9.8% are mounted on the bottom wall in front the model, spaced by a small set of transparent material in order to allow the illumination of the model lower region for detecting the stagnation point by PIV technique. The porous plates are connected via a transparent collector to a centrifugal pump. In order to evaluate the suction mass flow trough the porous wall, the static pressure step between the test section and the collector has been measured. For this purpose 4 pressure ports are located on the porous walls and 6 pressure taps are mounted on the side walls of the collector.

Figure 4: CT-1 wind tunnel

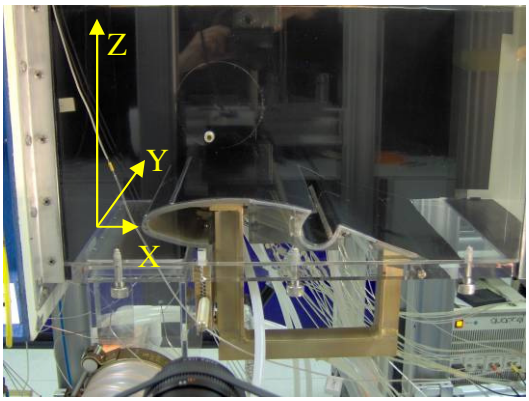

Figure 5: Test bed mounted on the WT bottom wall

2.2 Test article

The model represents a two dimensional airfoil, it is characterized by a chord length of 350mm and a spanwise length of 305mm. The model angle of attack (AoA) ranges between 5.66° to 12.66° with a step of 1°. The cavity shape has been designed starting from the data of the pressure surface distribution measured on the clean airfoil and by a numerical potential code as described by Cherniyshenko and other 2007.

The TVC has been designed and built in order to apply inside the cavity flow suction and blowing. The internal zone of the cavity oriented toward the leading edge presents 906 passing holes with a diameter of 1mm. These holes are connected to three different collectors in order to apply different suction mass flow values. Each collector is singularly connected by dedicated circuit to a vacuum pump. Each circuit is equipped with a partial valve in order to vary the mass flow rate and with a flow meter for measuring and storing the data. Hereinafter the suction regions shall be named as CAV1, CAV2 and CAV3. The backward zone of the cavity presents 126 passing holes of 1 mm diameter connected to a collector as well. From here the mass flow is injected. The holes have been designed as much as possible tangential to the cavity surface. The blowing collector is supplied by pressurised compress air via an independent circuit equipped by partial valve and flow meter devise. The blowing region in the following shall be indicated as CAV4. The geometry of the trapped cavity and the location of the suction and injection porous region are described in fig. 6.

The model is equipped with 37 pressure taps (PTS), 33PTS longitudinal spaced and 4 PTS spanwise located inside the TVC. Figure 7 shows the model geometry at 7.66° of AoA with the longitudinal PTS locations. The cavity has been instrumented by 15 PTS in order to monitor the behaviour of the vortex flow.

The vortex cavity has been realized by transparent material in order to allow the illumination of the flow region inside the cavity and perform PIV measurement.

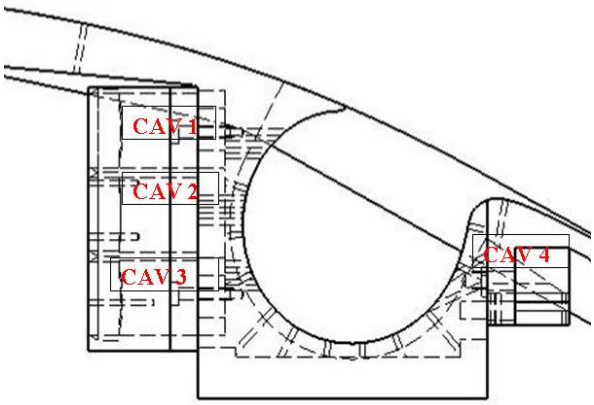

Figure 6: TVC drawing

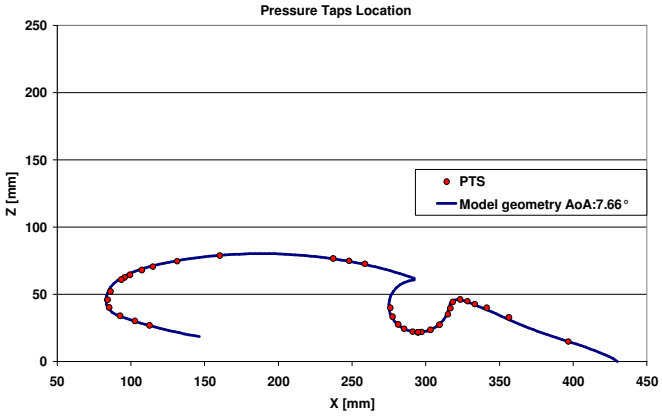

Figure 7: Model geometry with PTS location

2.3 Measurement instrumentations

The values of the pressure taps located on the model test-bed and the static pressure in the test section upstream the model have been acquired by means of the Hyscan 2000 system. Pressure taps were connected to a Scanivalve ZOC 22B electronic pressure scanner, characterised by: full scale ranges of ±1 psid, an accuracy value of ± 0.15% F.S., Scan Rate value of 20 kHz and Temp. Sensitivity of 0.05 %F.S./°C.

The flow field measurements have been carried out by means of Particle Image Velocimetry technique. The recording region is illuminated by two Nd-Yag resonator heads providing a laser beam energy of about 300mJ each at a wave length of 532 nm.

In order to measure simultaneously the upper and lower region of the model and in particular for illuminating the flow field inside the cavity a double light sheet configuration has been adopted. The laser beam, after the recombination optics is split in two beams. The beams are directed inside two different mechanical arms, each composed by seven mirrors and able to provides six freedom degrees. The arms can deliver the beams up to a distance of 2 meters from the laser. At the exit of the arms a set of lens (spherical and cylindrical) provides to open the beam in a light sheet and to focalise at the requested distance. The understanding of the TVC flow behaviour drove to measure the flow velocity inside the cavity. One of the difficulties coming from the experimental set up was the optical access to the cavity. The geometrical shape presented two main problems; absence of optical access, solved building the cavity model by transparent material, strong reflection due to the convex shape solved illuminating the cavity passing trough the model bottom minimising the reflection on the cavity surface. The model illuminated from both directions is shown in figure 8.

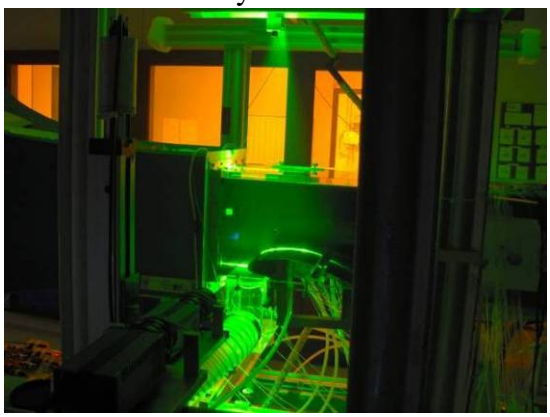

Figure 8: Illumination system

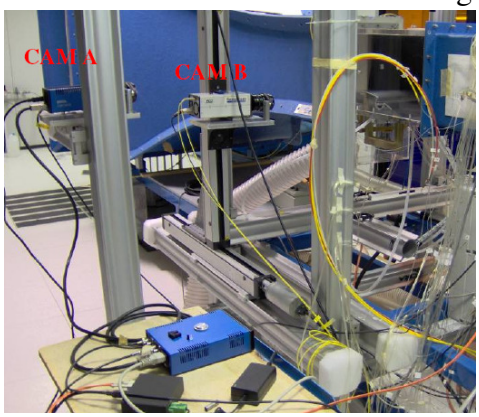

Figure 9: Recording system

The recording system has been improved. CCD cameras with higher pixel resolution have been used (2048x2048 px). Two cameras have been used and mostly simultaneously. One camera mounted a 100 mm lens providing a measurement area of about 65x65 mm^2 and higher spatial resolution (0.5 mm/vector). This camera has been used for measuring the vortex in the cavity and the flow field close to the model surface. In order to allow a fine positioning, the camera has been mounted on a 2D linear traversing system remotely controlled. This camera is indicated as CAM B. The second camera has been mounted on an optical bench at larger distance from the model. The camera mounted a 60mm focal lens and acquired a wider region of the order of 270 x 270 mm^2 characterised by a spatial resolution of 2.1 mm/vector. The second camera was aimed to measure the external flow above the full model. Hereinafter this camera is named CAM A. Figure 9 shows the recording set up. The image focusing was adjusted by means of a remote control system.

3. Experimental test

The measurements have been aimed to investigate the influence of the suction and blowing on the behaviour of the vortex inside the cavity and the influence on the external flow, i.e. if the trapped vortex was able to delay or even avoid the flow separation. The influence of different parameter has been investigated. Test have been performed varying the wind tunnel speed (15 m/s, 20 m/s, 25 m/s, 26.5 m/s, 28 m/s and 30 m/s), varying the mass flow suction (from 3 m^3/h to 25 m^3/h) varying the blowing mass flow (from 3 m^3/h to 50 m^3/h) applying suction and blowing at the same time, and varying the model angle of attach. Scope of the tests was also to individuate the minimum value of the blowing coefficient (Cμ) able to stabilize/trap the vortex in the cavity and induce the flow reattachment. Preliminary flow visualization tests using micro-taft demonstrated that for a wind speed of 15 m/s the flow is steady applying a flow suction in front the model of 0.096 kg/s corresponding to a pump speed value of 740 rpm, whereas at 30 m/s the flow is stabilised imposing 0.145 Kg/s suction mass (1100 rpm). Imposing the above mentioned mass flow values, the vortex shedding from the lower part of the model leading edge area was eliminated. Once stabilised the basic flow, the bi-dimentionality of the experiment has been verified performing PIV measurement on parallel horizontal planes. The position of the horizontal planes is shown in figure 10.

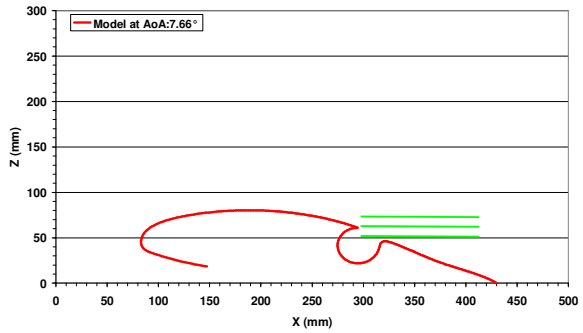

Figure 10: Horizontal Illumination system

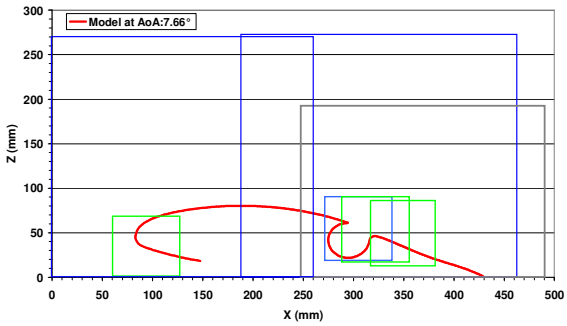

Figure 11: Recording system

PIV measurements have been performed on the vertical plane of symmetry of the test section long the main flow direction. Different regions have been recorded with different magnification factors. Figure 11 shows the zone acquired by both cameras. Global overview of the flow field has been detected by CAM A recording three different regions. Details of the flow has been detected by the CAM B, and in particular the lower front region where the stagnation point is located, the region inside the cavity for measuring the trapped vortex and the region immediately downstream the cavity for verify if flow reattachment occured. For each test condition together with the PIV images the model pressure data, the wind tunnel data (in term of wind speed, total temperature (T_0), total

pressure (P_0), and dynamic pressure), the static pressure drop on the porous wall and the mass flow values applied inside the cavity have been recorded.

4. Data processing

In this section the data processing is described. Together with image pre-processing and image analysis, the procedures adopted in order to: evaluate the steadiness of the flow separation, to detecte the flow separation and stagnation point locations, the position of the centre of the vortex, the extrapolation of the tangential and radial velocity components and the interaction with the external shear layer are described.

4.1 PIV images pre-process and analysis

For each test condition al least 150 couples of PIV images have been acquired. The images have been filtered by subtracting the minimum image calculated on the complete set of image samples for test case. This pre-process function allows reducing the background noise of the PIV images and increasing the signal to noise ratio. Moreover all the recordings acquired on the model have been masked for increasing the results reliability close to the model surface. The images have been analysed by means of PivView 2C v2.46 software. The selected analysis algorithm was ***Multigrid interrogation*** for all the PIV images. The algorithm uses a pyramid approach by starting off with larger interrogation windows (128 x 128 px) on a coarse grid and refining the windows (down to 32 x 32 px) and grid (16 x 16 px) with each pass. For each test condition all the single velocity fields have been evaluated. From the instantaneous velocity fields the ensemble average velocity field, the root mean square (rms) and the relative turbulence level (RTL), have been calculated. Furthermore out of plane component of the vorticity, shear stress and normal stress have been evaluated.

4.2 Data post processing

Once the velocity field has been evaluated, for detecting the flow separation position has been developed a dedicated routine. Starting from the first point of the geometry of the model where PIV data have been detected, the tangential velocity is calculated along the orthogonal direction to the surface. The tangential velocity is calculated by interpolating the closer neighbours. When reverse flow is detected a control is performed on the first and second derivative and on the tangential velocity for at least three more positions downward in order to validate the separation point. The separation point has been measured on the average velocity field and on each single velocity field in order to evaluate the flow unsteadiness.

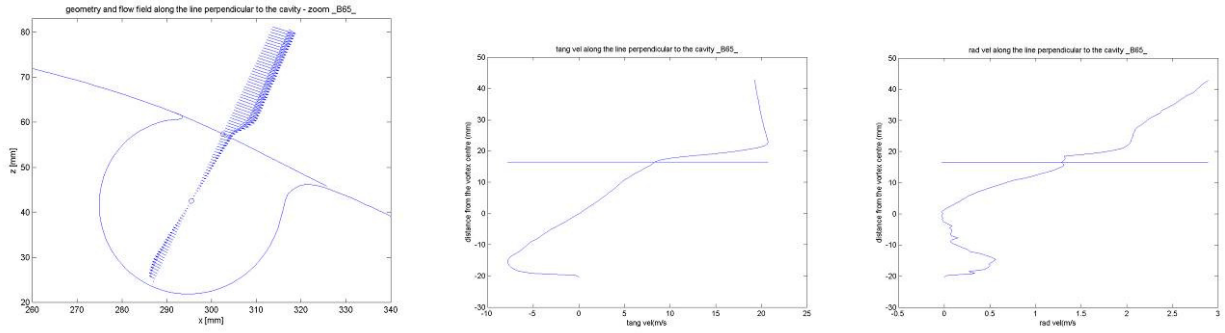

Figure 12: PIV recording set up on the LE

By analysing the flow field in the region under the front part of the model the stagnation point position has been detected on the ensemble velocity field results in analogous way. The behaviour of the vortex in the cavity and the influence on external flow has been further evaluated. The vortex centre position has been detected, the vorticity intensity and the circulation is calculated. Starting

from the vortex centre, the tangential and radial velocity is calculated along the line passing trough the vortex centre and orthogonal to the ideal polynomial curve that connect the tip of cavity with the downstream surface (figure 12). The velocity behaviour provides clear information of the interaction between the external flow and the internal vortex.
The values of the pressure distribution are presented in terms of pressure coefficient Cp defined as: $C_P = \frac{p - p_\infty}{q}$ where $q = \frac{1}{2}\rho V_\infty^2$ is the dynamic pressure obtained by the WT data acquisition system, p is the pressure on the model and p_∞ is the static pressure to the test section entrance.
The influence of the suction and blowing mass flow in the cavity is defined by dimensionless magnitude, the blowing coefficient (Cμ), defined as: $C_\mu = \frac{T}{qS} = \frac{\dot{m}V}{qS}$, where T is the thrust, S is the model surface, $\dot{m}$ is the mass flow suction/blowing in the cavity measured by the flow meters and V is the flow speed trough the cavity porous regions (CAV1,2,3 and 4).

4. Results and discussions

In the following the main results are presented and discussed. As it is possible to deduce from the tests description from the previous section, a considerable amount of data was acquired. So far, in the following only an overview is reported. PIV measurement system has been utilised in order to verify the bi-dimensionality of the experiment. The flow field has been cut with three horizontal PIV planes respectively at Z=51mm, 61mm and 71mm in proximity of the TVC for a WT speed of 15 m/s, suction pump speed of 740 rpm and model AoA of 7.66°. The u and v component of the velocity field has been measured.

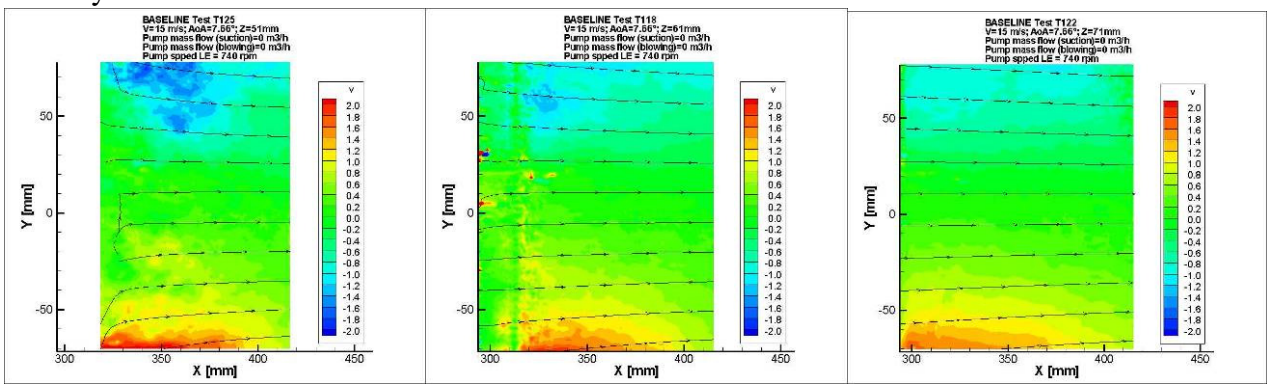

Figure 13: v-component on horizontal plane at: z=51, 61 and 71mm, AoA: 7.66°, vel:15m/s, pump: 740 rpm.

Figure 13 shows the v-component of the velocity as colour map for the three measured planes. The results show the presence of a transversal velocity component on the upper and lower sides of the image due to the wall effect. The flow in the central region, where the measurements have been conducted, can be considered bi-dimensional.
The flow instability induced by the flow trapped between the lower front part of the model and the bottom wall has been removed suctioning the mass flow in front the model. In figure 14 are reported, on the left side the flow field around the clean model measured in the close test section, where a strong circulation flow is visible below the airfoil leading edge, on the right side the flow field around the model equipped with the trapped vortex where the flow suction trough the bottom wall has been applied. In this second case the results show that the circulation region has been removed. Further confirmation is provided by the stabilization of the separation point location.

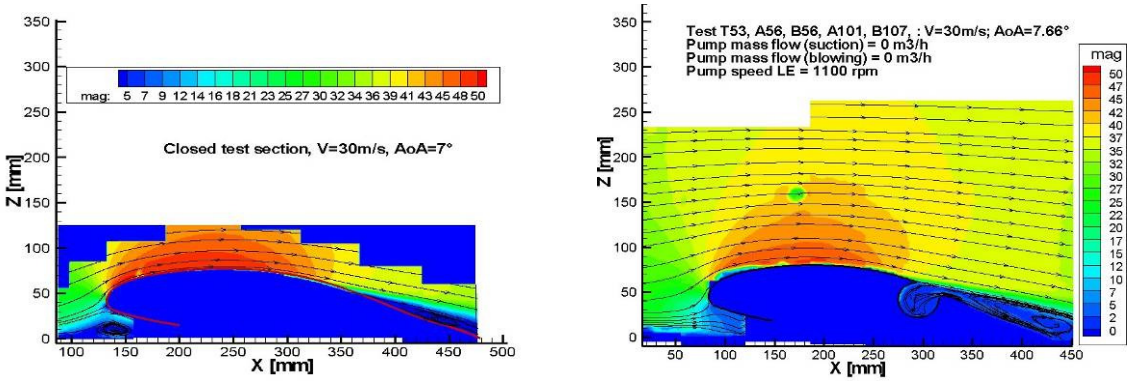

Figure 14: Flow field without suction in front the model(left) and with suction (right)

The influence of the TVC on the model without mass transfer has been investigated for different WT speed (from 15 to 30 m/s) and different angle of attack. For all the cases the flow field and the pressure coefficient showed that the flow separates from the cavity tip and do not reattach downstream the cavity. This effect is more pronounced as the wind speed or the AoA increases. For this reason the attention has been focused to the lower velocity (15 m/s). Figure 15 reports the flow field behaviour inside the cavity and immediately downstream the airfoil surface for same wind speed 15 m/s and for six different values of AoA (A=5,66°, B=6.66°, C=7.66°, D=9.66°, E=10.66° and F=12.66°).

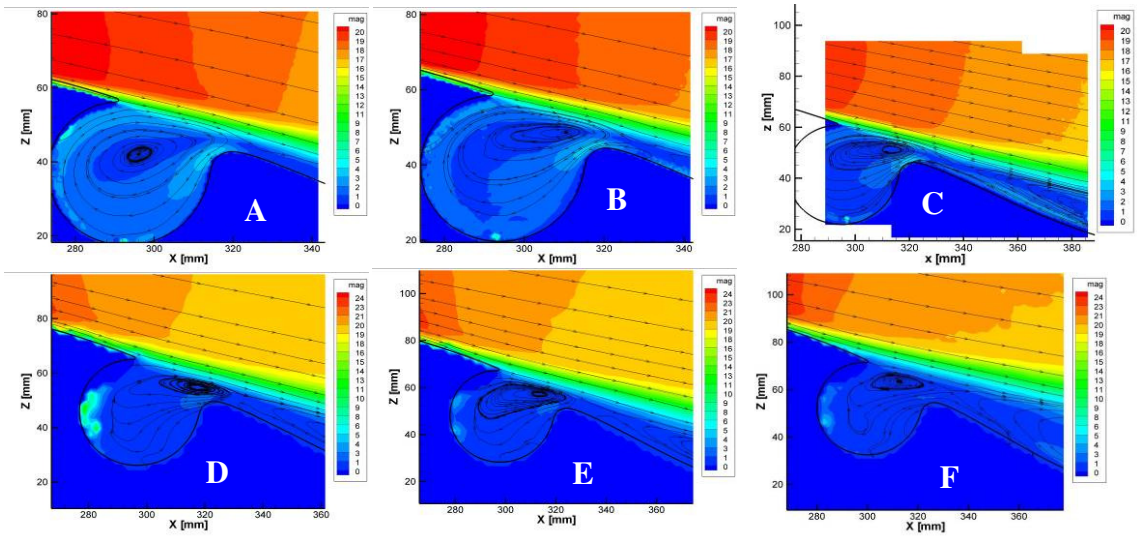

Figure 15: Flow field velocity inside the cavity without suction/blowing mass flow

The velocity magnitude colour map and the flow stream lines show for the smaller angle (5.66°) a weak vortical structure in side the cavity, with the centre located far from the geometrical centre and moved toward the shear layer region, the shape of the vortex is stretched toward the exit of the cavity. The vortex strength is not sufficient to force a flow reattachment. As the AoA increases the vortex centre move toward the shear layer region and it is suck out side the cavity inducing further vortex shedding. Flow from the downstream separated region is sucked inside the cavity. Figure 16 shows the Cp distribution of the longitudinal pressure taps long the model chord for different values of the AoA (from 5.66° to 12.66°). Let note that the pressure taps in the cavity are located between 54% and 66% of the model chord. The Cp values show the typical pressure distribution behaviour with a clear expansion on the upper leading edge region up to a maximum value for later start the pressure recovery until to encounter the cavity region. Here in the cavity the CP value shows a plateau behaviour meaning that the flow is mainly separated and unsteady. Mowing downward the cavity, pressure value continues to remain constant indicating that the flow is full separated. In

figure 17 the values of the tangential velocity in the cavity varying the angle of attack are reported. As already noted, the intensity of the velocity is really weak, only for the angle 5.66° and 6.66° is possible to individuate the typical behaviour of a vortical structure.

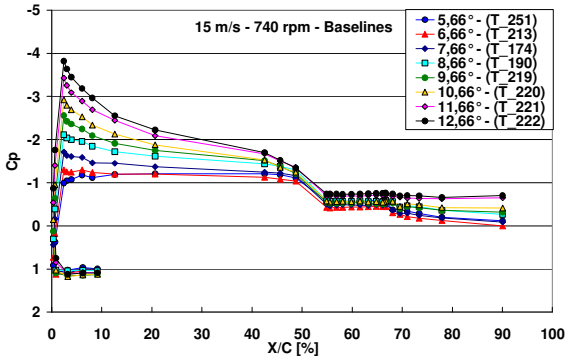

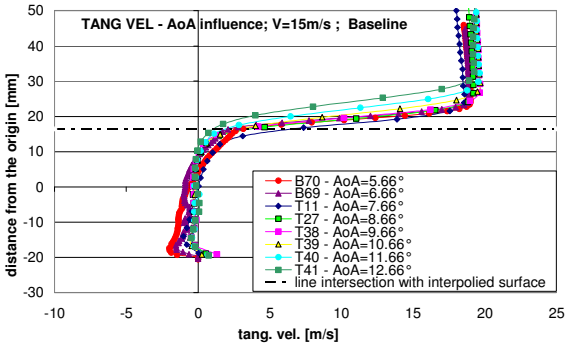

Figure 16: Cp distribution varying the AoA for V=15m/s **Figure 17: Tangential velocity inside the cavity**

Active flow control has been applied imposing flow suction inside the cavity in order to stabilise the vortex. Different values of mass flow have been applied. Figure 18 shows the velocity field inside the cavity for the following values of mass flow and blowing coefficient (Cμ) (Image A $\dot{m}$ =4.5 m3/h and Cμ=0.000189, image B $\dot{m}$ =9 m3/h and Cμ=0.000756, image C $\dot{m}$ =15 m3/h and Cμ=0.0021 and image D $\dot{m}$ =25.4 m3/h and Cμ=0.0059). The case A, characterised by the lowest value of Cμ, shows a small improvement respect the baseline, the applied suction is not enough to impose flow reattachment. Increasing the suction to a value of 9 m3/h, the flow is forced to reattach for a while for separating again to the 75% of the chord. In this case the trapped vortex is stable inside the cavity and the vortex centre is located almost in the geometrical centre of the cavity. Further increasing the value of Cμ, case C and D, the vortex strength increases and induce a full reattachment of the flow to the end of the airfoil.

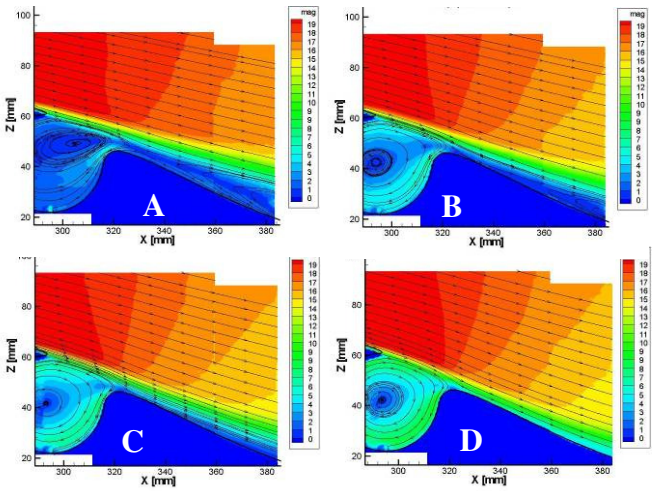

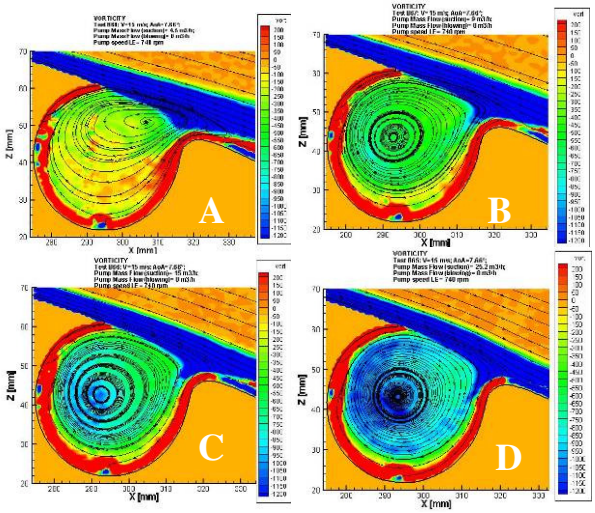

Figure 18: Velocity magnitude varying flow suction. **Figure 19: Vortiticy varying flow suction.**

This effect is clearly visible by the increment of the velocity magnitude in the cavity and by the reattachment of the stream lines. In order to provide a better understanding of the vortex strength in figure 19 the correspondent vorticity values are also reported.

In figure 20, the Cp behaviours for the baseline condition, i.e. without any mass transfer, and the cases with different flow suction values are reported. Respect the baseline diagram the Cp distribution for the case of 4.5 m^3/h (Cμ=0.000189) presents an increment of Cp immediately ahead the cavity, indicating a flow velocity increment induced by the presence of the vortex. The Cp values in the cavity are still flat but shifted toward higher values in absolute terms, meaning that the flow velocity in the cavity is higher. The values of Cp downstream the cavity do not show a

pressure recovering, indicating that the flow is still separated as shown by the PIV measurements. Increasing the suction to 9 m^3/h (Cμ=0.000756), the Cp behaviour shows the same trend in front and in the cavity but a clear pressure recovering downstream the cavity due to the flow reattachment. This tendency is more accentuated as the mass flow suction increases, case of 15 m^3/h and 25.4 m^3/h.

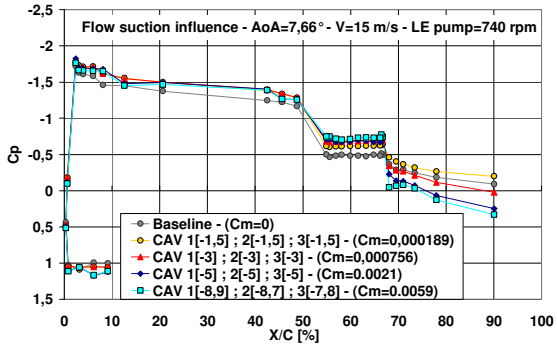

Figure 20: Cp distribution varying the Cμ V=15m/s

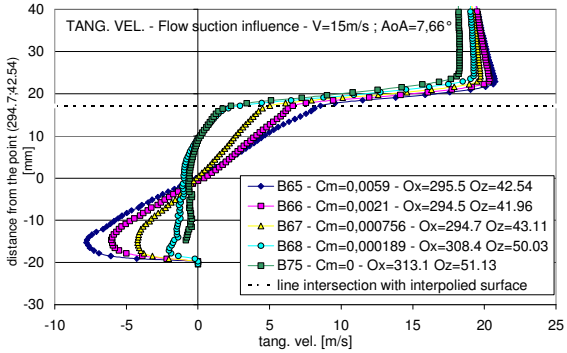

Figure 21: Tang. Vel. inside the cavity varying Cμ

Lets observe the case with maximum suction (Cμ=0.0059), in the diagram indicated by square light blue markers. The pressure value in the cavity do not present a constant behaviour, but it has convex curvature due to the significant value of the tangential speed. Furthermore pressure taps located at 68% of the cord, immediately downstream the cavity, presents a drop in the pressure coefficient with value close to zero. Probably we are close to the cavity stagnation point. Moving downward the CP value increases until the 73% of the chord for later decreasing again. The Cp distribution indicates that at 68% of the chord the flow velocity drastically decreases for re accelerates downstream pushed by the presence of the vortex for than decreasing as encounter the adverse pressure gradients. This behaviour is well documented in the figure 18 image D.

The influence of the wind tunnel velocity on the model with constant suction $\dot{m}$ =25.4 m3/h and for 7.66° incidence angle has been investigated. Starting from 15 m/s the velocity has been increased respectively to 20 m/s, 25 m/s, 26.5 m/s and 30 m/s. As consequence of the variation of the speed the blowing coefficient is varied as well. Scope of the test was to individuate for a fixed value of the flow suction the limit speed for reattachment. The PIV results indicate 26.5 m/s as the upper limit speed for allowing the flow reattachment, corresponding to Cμ=0.00184. The Cp distribution is reported in figure 22. The diagram indicates that for the cases with wind speed from 15 to 26.5 m/s the Cp downstream the cavity presents a pressure recovery, behaviour that is not present for the case relative to the speed of 30 m/s, where the flow is still separated.

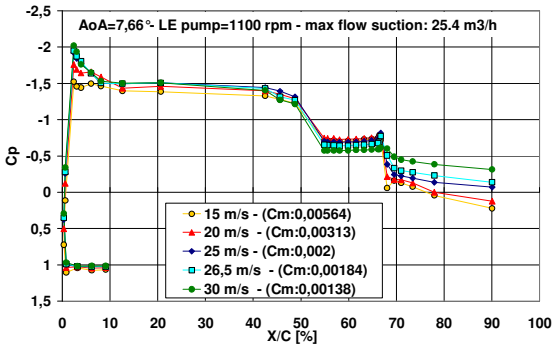

Figure 22: Cp distribution varying the WT speed

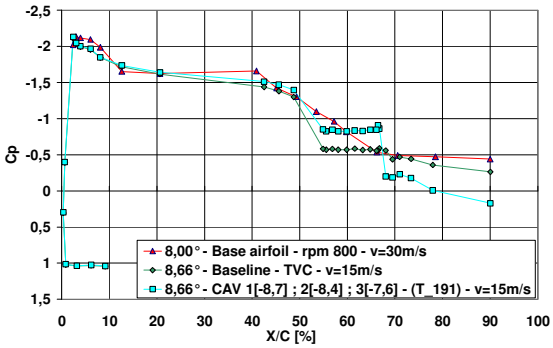

Figure 21: Cp distribution for clean, TVC baseline,

A final statement is not possible to be done at the moment but some conclusion can be extrapolated get comparing the Cp distribution related to: clean airfoil, airfoil with TVC and airfoil with TVC

and Cμ=0.0059. The comparison is shown in figure 21. The three different cases show almost the same maximum Cp value. The clean airfoil presents a flow separation at 70% of the chord. The TVC passive flow control is characterised by a flow separation from the cavity tip (54% of the chord) and globalilly the behaviour is worst of the clean configuration. The TVC active flow control for Cμ=0.0059 presents a flow fully attached with a noticeable decrement on the pressure drag.

5. Conclusions and future activities

An extensive test campaign has been successfully performed in order to investigate the potentiality of trapped vortex cavity flow control. The TVC has been investigated as passive and active method, i.e. without and with mass transport. The full pressure and flow characterization has been detected for the base clean airfoil and for the model modified for carrying the flow control device. A complex experimental set up has been realised composed by different elements: the suction system for removing the unsteady circulation region in front the model, the suction/injection systems for active flow control in the cavity, the measurement system for recording all the boundary condition.
From the showed results the following conclusions can be draw. Passive TVC flow control is not able to control the flow separation. The vortex is not confined in the cavity and vortex shedding is present decreasing the aerodynamic characteristics of the original airfoil. Active TVC flow control is able to control the flow separation, for limited values of the blowing coefficient full reattachment has been obtained. These first experiments provided really encouraging result. The campaign shall provide unique experimental data to the numerical colleague for code validation. As future activities the project foresees that CIRA shall test the TVC concept in a large wind tunnel on a real 2D model wing in order to evaluate the benefit in terms of aerodynamic coefficients.

Acknowledgements

This work has been partially funded by European Commission in the frame work of the VortexCell2050 research project (contract number AST4-CT-2005-012139). The authors wish to acknowledge the valuable contributions enabling the success of this investigation by Prof. S. Chernyshenko for the efforts in the VCELL co-ordination, and dr. R. Donelli in co-ordinating the internal CIRA activities.

References

Gad-el-Hak, M. (1996) Modern development in flow control. Applied Mechanics Reviews, vol. 49, pp. 365–379.

Ringleb F.O. (1961). Separation control by trapped vortices. In: Boundary Layer and Flow Control, Ed. Lachmann G.V., Pergamon Press.)

Kasper W.A. Some Ideas of Vortex Lift. Society of Automotive Engineers, Inc., Warrendale, PA, Paper 750547, no date, pp 12

Kruppa E.W. (1977) A Wind Tunnel Investigation of the Kasper Vortex Concept. AIAA, Paper 77-310, pp. 10

De Gregorio F., Albano F., Lupo M., (2007) Flow separation investigation by PIV technique, proc. of 7th International Symposium on Particle Image Velocimetry, Sept. 11-14, 2007 Rome, Italy.

Chernyshenko S., Donelli R., Iannelli P., Iollo A., Zanetti L., (2007) Flow models for a Vortex Cell, submitted to AIAA Journal

Adrian R.J., (1991) Particle imaging techniques for experimental fluid mechanics, Annual Review of Fluid Mechanics, Vol. 22, , pp. 261-304.

Raffel M., Willert C.E. and Kompenhans J., (1998) Particle Image Velocimetry, Springer-Verlag